

Crystallographic Structure and Chemisorption Activity of Palladium/Mica Model Catalysts

III. Static Secondary Ion Mass Spectrometry Study of CO Chemisorption on Small Palladium Particles

V. MATOLIN,¹ E. GILLET, AND S. CHANNAKHONE

Laboratoire de Microscopie et Diffractions Electroniques, UA 797, Faculté des Sciences et Techniques de St-Jérôme, Rue Henri Poincaré, 13397 Marseille Cedex 13, France

Received July 20, 1984; revised July 23, 1985

The application of static secondary ion mass spectrometry (SSIMS) to the surface investigation of small supported palladium particles is described. The method is applied within the frame of a catalytic reaction study (CO oxidation). The secondary ion yields are measured during CO adsorption and desorption. It is shown that it is possible to identify two states of CO bonding and to make quantitative measurements of adsorbed amounts in relation to previous thermal desorption results. The effects of heating treatments in CO + O₂ mixtures are investigated for various particle sizes.

© 1986 Academic Press, Inc.

INTRODUCTION

Several studies of model supported metal particle catalysts in CO oxidation have recently been reported from different laboratories (1-4). These studies have shown that CO adsorption-desorption and catalytic reaction mechanisms on small particles are a very complex problem, since they are often significantly affected by the particle structure, morphology, and size which can change during the gas treatment (2-4). In Parts I and II (3, 4) we presented results obtained by transmission electron microscopy (TEM), transmission electron diffraction (TED), and temperature-programmed desorption (TPD) studies. We showed the changes occurring in "as-deposited" small Pd particles, during gas treatment in the CO + O₂ atmosphere, toward the stable morphology. We also showed the existence of two types of CO adsorption states depending on particle morphology and the possibility of dissociative CO adsorption on small

Pd particles. This is an idea that has also been mentioned by other authors (2), but which must still be confirmed.

To investigate a model catalyst, it is essential that the crystallographic, adsorption, desorption, and reaction studies be accompanied by the analysis of the surface layers. In the case of small particles the electron spectroscopy methods (AES, ESCA, EELS) commonly used to analyze homogenous surfaces give results whose interpretation is difficult. This is due to the contribution of the particle support to the analyzed signal.

In the case of catalytic reaction studies, it would be interesting to monitor directly the presence of the molecularly adsorbed CO, and other species, on the particle surface (separately from the support surface) during the reaction. Furthermore it is important to separate the dissociative CO adsorption, which was observed in the case of the small Pd particles (2, 3), from the molecular absorption.

Unsatisfactory results for electron spectroscopy methods in surface analysis of small supported particles have led us to uti-

¹ Permanent address: Department of Electronics and Vacuum Physics, Charles University, Povltavska 1, 18000 Prague 8, Czechoslovakia.

lize another method, namely, static secondary ion mass spectrometry (SSIMS), which has previously been used for surface studies on massive crystals. In this article, we would like to show that this method can be a powerful tool in the surface investigation of a model small-particle supported catalyst.

In 1973, Benninghoven showed that it is possible to investigate surface reactions by the so-called "static" method of SIMS the typical feature of which is the bombardment of a relatively large target area with a relatively low primary ion current density (5). At 10^{-9} A cm^{-2} with an emission yield of secondary particles of one per incident ion, for example, it takes about half an hour to remove 1% of a monolayer. Thus, although each ion impact damages a small region of the surface, the contribution of previously damaged regions to the observed spectrum can be negligible. To determine the kinds of information that SSIMS can provide for surface analysis, one must focus on the collision process itself. The central issue is establishment of relationships between measured SIMS parameters and the structure and chemistry of the surface (6).

Recently, several authors have shown that SSIMS studies can be successfully applied to the investigation of the structure in the CO adsorption layer on Ru(111), Ni(111), Ni(100) (7-10); on polycrystalline Pd and Ag (11); on Pt and Cu (10); and on Pd(111) (7). It was shown that molecular adsorption of CO on the metal surface is characterized by the appearance of the ion cluster species $M_n\text{CO}^+$ in the secondary ion spectra, while the $M_n\text{C}_m^+$ species are characteristic of dissociative CO adsorption.

An empirical approach to the application of SSIMS signals for CO coverage studies has been necessary. It was shown that there exists a relationship between the sum of the SIMS intensity ratios and the coverage θ (7-8):

$$\sum_n \frac{\text{Pd}_n\text{CO}^+}{\text{Pd}_n^+} = f(\theta).$$

The advantage of using intensity ratios rather than the absolute values of these intensities is to cancel out the effect of the work function variation during the adsorption. It was demonstrated that this relationship is linear, except for the change in slope which was observed in several systems, and that it was correlated with adsorbate structure variations during the adsorption.

More recently Brown and Vickerman (7, 8) have shown that the "mass spectrum" of molecularly adsorbed CO also contains information about the site geometries. Thus "linear," "bridged" and "threefold" bonded CO are characterized by specific relative yields of $M\text{CO}^+$, $M_2\text{CO}^+$, and $M_3\text{CO}^+$. In the case of linear $M\text{CO}$ sites the probability of emission of ion clusters $M_2\text{CO}^+$ and $M_3\text{CO}^+$ is low with respect to the probability of emission of $M\text{CO}^+$, and the ratio $M\text{CO}^+ / (\sum_n M_n\text{CO}^+) \approx 1$. For bridged and threefold bonded CO all ion clusters $M_n\text{CO}^+$ occur in the SIMS spectrum and the fragmentation pattern $M\text{CO}^+ : M_2\text{CO}^+ : M_3\text{CO}^+$ can be defined.

EXPERIMENTAL

The studies were performed in the two-chamber type UHV system described in Part II (4).

Pd particles were grown on cleaved mica substrate by evaporation *in situ* from a Knudsen cell in the analytical-preparation chamber equipped for SIMS experiments. The particle samples were prepared at various substrate temperatures (550 to 590 K) and various Pd exposures in order to achieve an average particle size in the range of 2-10 nm. The surface cleanliness of as-deposited samples was monitored by SSIMS.

Particle structure, size, and morphology were investigated by TEM and TED as well as by changes due to annealing in various atmospheres during experiments of adsorption and desorption and catalytic reaction (3). Catalytic reactions were performed in a separate reaction chamber, equipped for TPD experiments, which could be isolated

from the analytical-preparation chamber (4).

The SIMS studies were performed using a quadrupole mass spectrometer, with range of 1–300 a.m.u. and an ion energy filter, and an ion gun with differential pumping. The primary ion source provides a beam of argon ions with energy up to 5 kV and the incident angle on the sample plane is 45 degrees. The experimental conditions were examined in order to optimize signal intensities and to minimize damage caused to the particle surface during the analysis. Thus the experiments were carried out at low resolution to increase spectrometer sensitivity and a low primary ion current density was used (5 to 10×10^{-9} A cm^{-2} at 600 eV), such that the crystallographic and chemical integrity of the surface layer was preserved during the period of study. The conservation of the integrity of the surface was verified on the one hand by the stability of the SIMS signals and on the other hand by TEM investigations of the particles before and after SSIMS studies.

The sample electrostatic charge, due to the polarization of the mica support during the ion impact, was neutralized by a low energy electron beam of 200 eV.

RESULTS AND DISCUSSION

Composition of the Surface Layers

Figure 1 shows a SSIMS spectrum relative to "as-deposited" small particles together with their mica substrate. The large signals of Na^+ , Al^+ , K^+ , Si^+ , Ca^+ , Fe^+ , and O^+ are due to the mica support. Simultaneously the ions Pd^+ and the ion clusters Pd_2^+ , PdCO^+ , Pd_2CO^+ , and PdK^+ are of significant intensity. The appearance of the Pd–CO ion species was due to the exposure to a background pressure of CO. If carbon contamination of the Pd particle surface occurred during the experimental run, the SSIMS spectrum exhibited the corresponding ion cluster species PdC^+ , Pd_2C^+ , and PdC_2^+ .

The relatively high intensities of the

PdK^+ signal were probably due to the high SIMS sensitivity for PdK species whose origin is mainly in the contamination of the surface in the region of contact between Pd particles and mica support. This is demonstrated by the observation of an increase in the PdK^+/Pd^+ ion ratio with decrease in the particle size. As no correlation was observed between the PdK^+ ion intensities and the results of the TPD and catalytic reaction studies, it seems that this contamination does not influence the CO adsorption and catalytic reaction properties.

The spectrum in Fig. 1 also exhibits PdOH^+ ion clusters due to water contamination of the small particle surface. This contamination is caused by insufficient heating of the mica substrate in this case. We found that annealing of the mica substrate for 1 h at 580 K before Pd deposition is necessary to prepare small particles which are not contaminated by water vapor.

CO Adsorption on Particles Larger than 6 nm

The possible utilization of SSIMS in the investigation of CO adsorption on small Pd particles larger than 6 nm is shown in this section, combining SSIMS and TPD.

Before SSIMS and TPD experiments, the particle samples were stabilized by thermal treatment in oxygen and a CO atmosphere (5×10^{-7} and 5×10^{-8} Torr, respectively) at 570 K to obtain a stable particle structure, size, and morphology (4). No contamination (except by CO) of the particle surface was observed by SSIMS during the experiments. This fact was confirmed by TPD results because no variations of the area under the TPD peaks of a CO-saturated surface were observed during the studies.

A clean Pd particle surface was exposed to increasing doses of CO at 300 K and 5×10^{-9} Torr. After each exposure a TPD spectrum was recorded with a linear heating rate of 3.6 K s^{-1} . The area S under the TPD peaks was used to obtain relative coverage

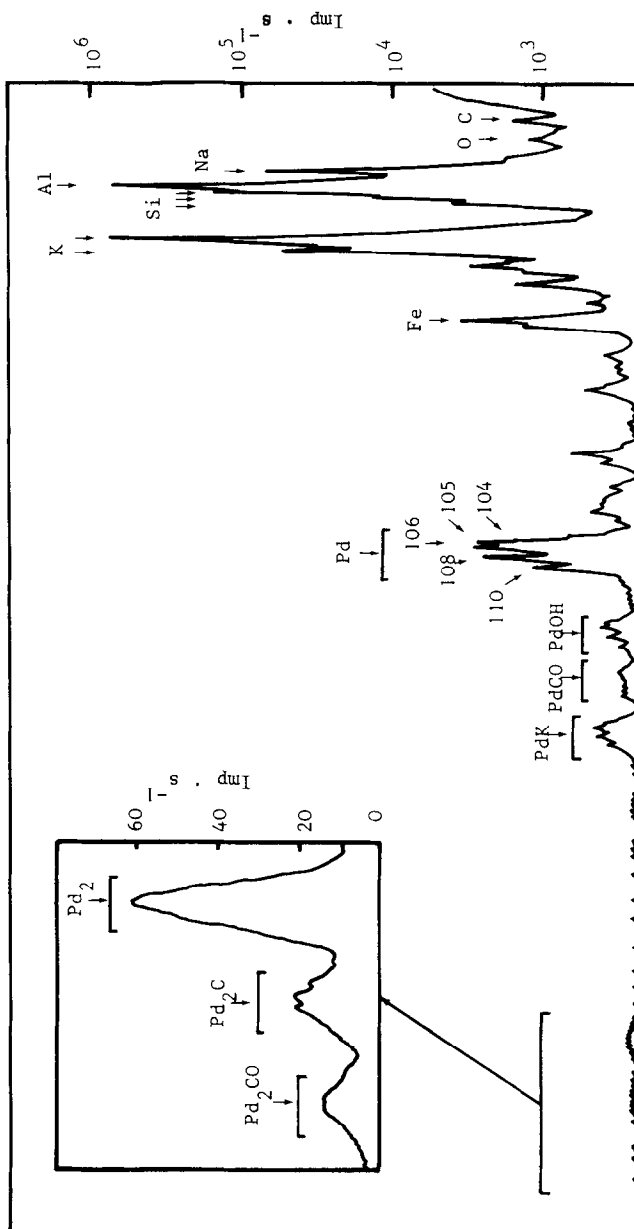


FIG. 1. SSIMS of small Pd particles on mica.

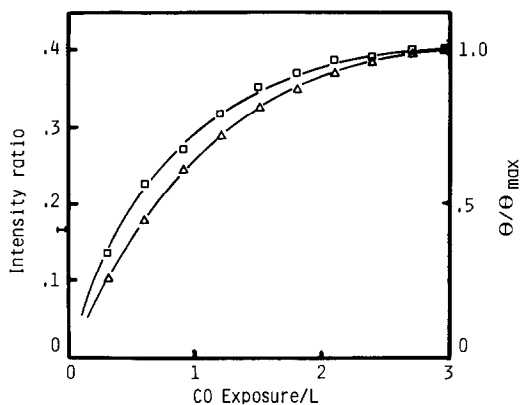


FIG. 2. Relative CO coverage (Δ) and sum of ion intensity ratios $\Sigma_n^2(\text{Pd}_n\text{CO}^+/\text{Pd}_n^+)$ (\square) as a function of CO exposure.

measurements θ/θ_m versus the CO exposure E (Fig. 2). After this procedure the sample was exposed to 5×10^{-9} Torr CO pressure at 300 K. During this exposure SSIMS data were recorded as a function of exposure. Adsorption of CO produced an immediate increase in the intensities of Pd_n^+ and Pd_nCO^+ species.

The variations in the Pd^+ intensity and in the sum of ion intensity ratios, $\text{PdCO}^+/\text{Pd}^+ + \text{Pd}_2\text{CO}^+/\text{Pd}_2^+$, are also presented, as a function of exposure E , in Fig. 2. We can see that Pd^+ and $\Sigma_n(\text{Pd}_n\text{CO}^+/\text{Pd}_n^+)$ intensities and θ/θ_m saturate together at 3 L exposure. Combination of the data in Fig. 2 makes it possible to plot the relationship

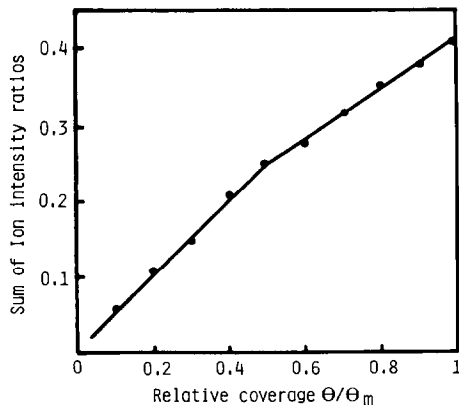


FIG. 3. Plot of the sum of ion intensity ratios $\Sigma_n^2(\text{Pd}_n\text{CO}^+/\text{Pd}_n^+)$ vs relative CO coverage θ/θ_m .

between the sum of ion intensity ratios and the relative coverage θ/θ_m , and this is demonstrated in Fig. 3.

The plot in Fig. 3 shows that this relationship is linear with a small slope change at about $\theta/\theta_m = 0.5$. The combination of TEM and TPD makes it possible to determine the value $\theta_m = 0.5$ (the total number of adsorption sites was calculated from particle size and density assuming a hemispherical shape for the particles and Pd(111) plane atom density), so it is seen that the slope change occurs at $\theta = 0.25$. The slope variation has also been observed on the bulk metal surface, and has been correlated with the change of the adsorbate structure (7, 10) during exposure.

In Fig. 4 we have presented the ion intensity ratio $\text{PdCO}^+/(\text{PdCO}^+ + \text{Pd}_2\text{CO}^+)$ as a function of θ/θ_m , and from this it is possible to deduce the site geometry of CO adsorbed on the surface of Pd particles as a function of CO coverage.

We can see that in the case of Pd particles with an average size larger than 6 nm the intensity ratio $\text{PdCO}^+/(\text{PdCO}^+ + \text{Pd}_2\text{CO}^+)$ was about 1 for low coverage. Since the fragmentation patterns of twofold site geometry (bridge) show that both

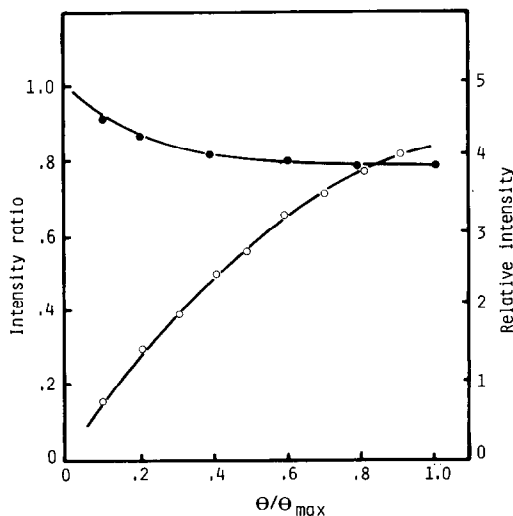


FIG. 4. $\text{PdCO}^+/(\text{PdCO}^+ + \text{Pd}_2\text{CO}^+)$ intensity ratio (\bullet) and Pd_2CO^+ (\circ) intensity vs θ/θ_m .

PdCO^+ and Pd_2CO^+ fractions must be present in the SSIMS spectra, the data in Fig. 4 suggest that only linear bonding can be found for low coverage on the small particle surface, because the Pd_2CO^+ must be about zero if the ion intensity ratio is about 1. The decrease in $\text{PdCO}^+ / (\text{PdCO}^+ + \text{Pd}_2\text{CO}^+)$ with increasing coverage of CO indicates a movement toward bridge bonding. A similar change was observed on the Pd(111) surface, and its relationship to appearance of bridge bonds was confirmed by IR spectroscopy in that case (7).

CO Adsorption on Particles Smaller than 5 nm

In Parts I and II (3, 4), we pointed out the complexity of CO adsorption on Pd small particles with regard to the variations in the particle parameters during thermal treatments with gases. For particles smaller than 5 nm, we observed that the area S under the TPD peaks decreases during adsorption-desorption cycles and increases

during heating in an oxygen atmosphere (2, 4).

This phenomenon was first interpreted as due to carbon contamination resulting from CO decomposition (2). In previous papers (3, 4) it was shown that the particle size and change of shape which occurs when the particles are heated in a CO + O₂ atmosphere contribute to the desorption peak area variations. We also reported that the desorption peak area reduction, probably associated with the carbon contamination, affects the small particles which exhibit a high energy desorption peak related to edge atoms, suggesting that a particular "bonding" is responsible for the CO decomposition.

In this section we will show that SSIMS combined with TPD results offers important information, which can contribute to the solution of these problems.

The freshly deposited sample was successively studied 11 times by TPD, always after saturation by CO (cycle A in Fig. 5).

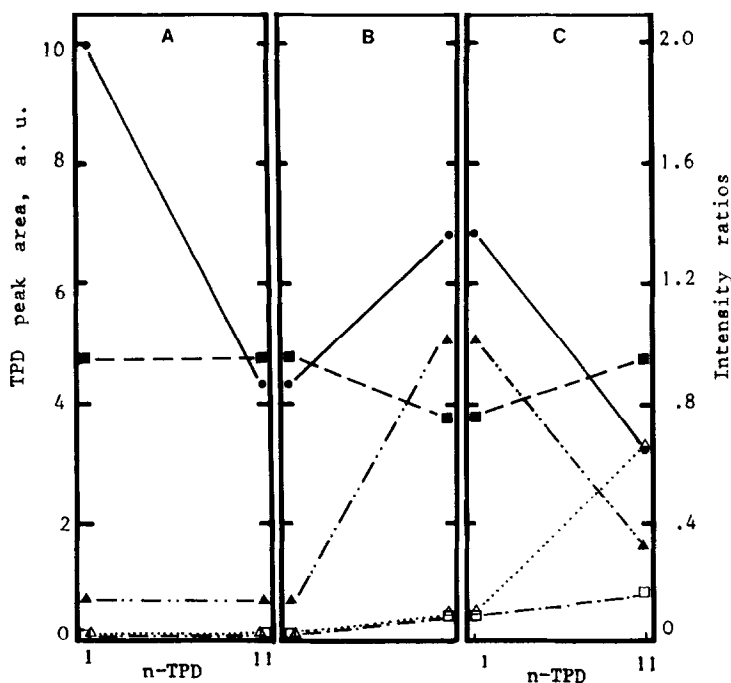


FIG. 5. Variation in TPD peak area S (●) and in the ion intensity ratios $\Sigma \text{Pd}_n \text{CO}^+ / \Sigma \text{Pd}^+$ (▲), $\text{PdCO}^+ / \Sigma \text{Pd}_n \text{CO}^+$ (■), $\text{PdC}^+ / \text{Pd}^+$ (□), and $\text{PdC}_2^+ / \text{Pd}^+$ (△) during cycles A, B, and C. (A) n adsorption-desorption ($n = 11$); (B) treatment (1 h) in O₂ + CO atmosphere at 570 K; (C) = (A).

After this process it was treated at 570 K, for 1 h, in an O₂ + CO atmosphere at 1×10^{-7} and 1×10^{-8} Torr of O₂ and CO, respectively (cycle B). After this treatment the sample was studied once more by 11 TPD runs (cycle C).

In Fig. 5 the relative variation of *S* (area under TPD peak) and the variations of the ion intensity ratios—PdCO⁺/Pd⁺ + Pd₂CO⁺/Pd₂⁺, PdCO⁺/(PdCO⁺ + Pd₂CO⁺), PdC⁺/Pd⁺, PdC₂⁺/Pd⁺—during cycles A, B, and C are shown, indicating the development of CO coverage, Pd–CO bonding, and carbon contamination. During cycle A, an important decrease in *S* occurs and no carbon contamination, and no change in the sum of Pd–CO ion intensity ratios is confirmed by SSIMS. These SSIMS data suggest that there is no variation in CO saturation coverage. The ratio PdCO⁺/(PdCO⁺ + Pd₂CO⁺) remains constant (about 1), indicating the existence of only linear site geometry. The decrease in *S*, which is plotted (in detail) in Fig. 6a (versus the number of TPD) is due to a decrease in the number of adsorption sites. This decrease can be correlated with the particle size distribution and shape changes resulting from particle coalescence and rebuilding (3). It is clear that the decrease in the number of adsorp-

tion sites is not due to carbon contamination.

During cycle B, an increase in *S*, an important increase in the sum of ion intensity ratios $\sum_n \text{Pd}_n \text{CO}^+ / \text{Pd}_n^+$, and a change in the site geometry are observed. These variations can be correlated with an increase in saturation coverage θ_m . Because no particle dispersion has been observed and the particles take a well-defined cuboctahedral shape (3), the increase in adsorption activity and the variation in site geometry can be correlated with particle faceting.

In cycle C an important decrease in TPD peak area (presented in detail in Fig. 6b) correlates with a decrease in the sum of ion intensity ratios, $\sum_n \text{Pd}_n \text{CO}^+ / \text{Pd}_n^+$, and therefore in the saturation coverage θ_m , and with an increase in the carbon contamination represented by PdC⁺/Pd⁺ and PdC₂⁺/Pd⁺ ion intensity ratios. The appearance of carbon on the Pd particle surface confirms the presence of CO decomposition during cycle C. At the same time there is a variation in site geometry toward linear bonding. Hence we can make the hypothesis that the carbon contamination affects the twofold coordination sites (bridge bonding).

SSIMS–TPD studies showed that gas treatment of the freshly prepared small par-

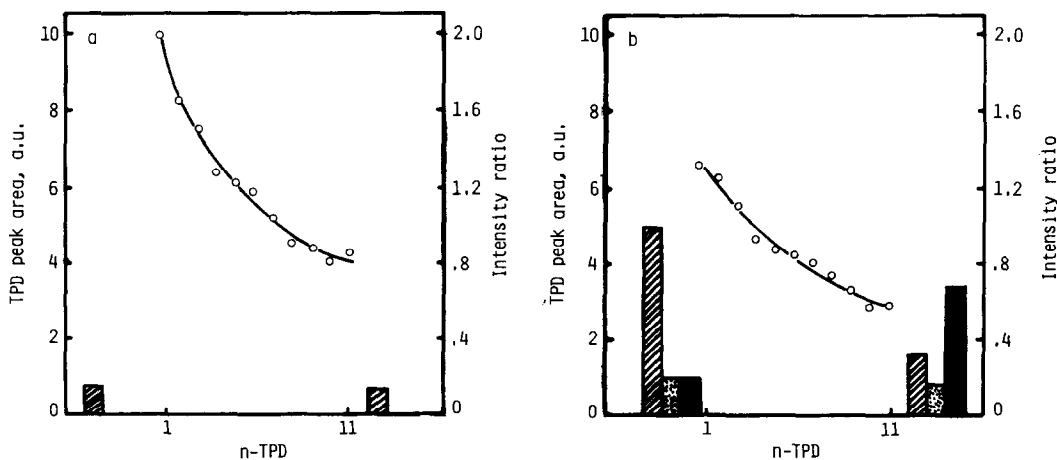


FIG. 6a,b Relative variation in area under TPD peak (○) and in ion intensity ratios $\sum_n (\text{Pd}_n \text{CO}^+ / \text{Pd}_n^+)$ (○), PdC⁺/Pd⁺ (▨), and PdC₂⁺/Pd⁺ (■) versus *n* TPD cycles (*n* = 1–11).

ticles of Pd produces important variations in the area under the TPD peaks. It has been shown that two principal reasons exist for the decrease in the number of adsorption sites, namely, CO decomposition on the particle surface and/or the size and morphological changes which result from particle coalescence. Another important result is suggested by the SSIMS investigation: the CO decomposition on small Pd particles not only depends on particle size but is also influenced by particle morphology.

CONCLUSIONS

We have shown that a SSIMS investigation of small particles in the size range 2–8 nm is possible. TPD, SSIMS, and TEM investigations showed that the ion bombardment did not have any important influence on the particle surface during the period of study.

SSIMS can be successfully used for particle surface analysis. Surface contamination, adsorption coverage, and type of bonding can be monitored before and during the adsorption experiments.

Adsorption of CO on the surface is represented by the appearance of the Pd-CO ion clusters in the secondary ion spectra. The results reported for the SSIMS study of CO adsorption on Pd particles with average size above 6 nm confirm the linear relationship between the sum of ion intensity ratios ($\text{PdCO}^+/\text{Pd}^+$) + ($\text{Pd}_2\text{CO}^+/\text{Pd}_2^+$) and coverage. In this way, the decomposition of CO is monitored by the presence of the Pd-C ion species in SSIMS signal.

In the case of small particles with an av-

erage size below 5 nm, the TPD-SSIMS studies show that CO adsorption is influenced by two principal processes. These are the size and shape changes of the freshly deposited particles when submitted to adsorption-desorption treatment, and the size- and morphology-dependent CO decomposition.

REFERENCES

1. Ladas, S., Poppa, H., and Boudart, M., *Surf. Sci.* **102**, 151 (1981).
2. Doering, D. L., Poppa, H., and Dickinson, J. T., *J. Catal.* **73**, 104 (1982).
3. Gillet, M., and Channakhone, S., *J. Catal.* **97**, 427 (1986).
4. Gillet, E., Channakhone, S., and Matolin, V., *J. Catal.* **97**, 437 (1986).
5. Benninghoven, A., *Surf. Sci.* **35**, 427 (1973).
6. Delgass, W. N., Lauderback, L. L., and Taylor, D. G., in "Chemistry and Physics of Solid Surfaces IV" (R. Vanselow and R. Howe, Eds.), Springer Series in Chemistry and Physics, Vol. 20, p. 51. Springer-Verlag, Berlin/New York, 1982.
7. Brown, A., and Vickerman, J. C., *Surf. Sci.* **124**, 267 (1983).
8. Brown, A., and Vickerman, J. C., *Surf. Sci.* **117**, 154 (1982).
9. Brown, A., and Vickerman, J. C., *Vacuum* **31**, 429 (1981).
10. Bordoli, R. S., Vickerman, J. C., and Wolstenholme, J., *Surf. Sci.* **85**, 244 (1979).
11. Slusser, G. J., and Winograd, N., *Surf. Sci.* **95**, 53 (1980).
12. Bradshaw, A. M., and Hoffmann, F. M., *Surf. Sci.* **72**, 513 (1978).
13. Schroer, J. M., Rodin, T. H., and Bradley, R. C., *Surf. Sci.* **34**, 571 (1973).
14. Sroubek, Z., *Surf. Sci.* **44**, 47 (1974).
15. Ertl, G., and Koch, J., in "Adsorption-Desorption Phenomena" (F. Ricca, Ed.), p. 345. Academic Press, New York, 1972.
16. Conrad, H., Ertl, G., Koch, J., and Latta, E. E., *Surf. Sci.* **43**, 462 (1974).